MEDIUM-β SUPERCONDUCTING ACCELERATING STRUCTURES*

J. R. Delayen†, Thomas Jefferson National Accelerator Facility,
Newport News, VA 23606, USA

Abstract

While, originally, the development of superconducting structures was cleanly divided between low-β resonators for heavy ions and β=1 resonators for electrons, recent interest in protons accelerators (high and low current, pulsed and cw) has necessitated the development of structures that bridge the gap between the two. These activities have resulted both in new geometries and in the adaptation of well-known geometries optimized for this intermediate velocity range. Their characteristics and properties are reviewed.

1 HISTORICAL BACKGROUND

Although one of the first proposals for the application of rf superconductivity to particle accelerators was for a ~1GeV, ~1mA proton accelerator [1], until the second half of the 1980's this technology was restricted to heavy-ion machines for nuclear structure studies and to high-energy electron machines. Success in these two applications generated interest in applying the superconducting rf (srf) technology to various high-current, high-brightness proton and deuteron accelerators that were under consideration [2].

As shown in Figure 1 the frequency-β region deemed of interest at the time was significantly different from the regions that had been explored for heavy-ion and electron accelerators.

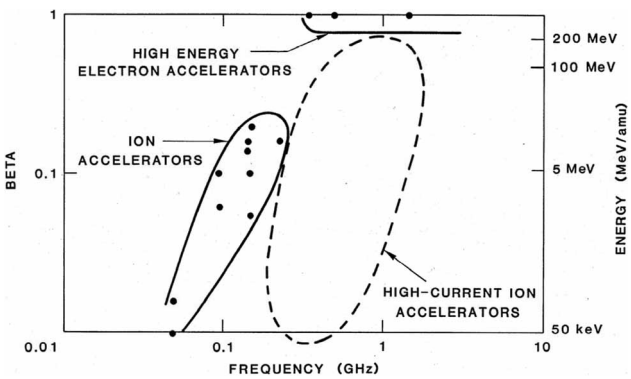

Figure 1: Frequency and β of interest for high-current ion accelerators, (circa 1988) [2].

There is no universal definition of what constitutes a medium-β cavity. In the low-velocity community a β=0.1 is often referred to as medium-β, while in the high-velocity it is applied to β~0.65. For the purpose of this paper the term medium-β will imply β roughly between 0.2 and 0.6.

Figure 2 shows a 1989 survey of all the low-β (which implied β<1 at the time) superconducting cavities that had been tested or were under development [3]. The medium-β region is virtually empty. The only structures that could be considered as medium-β were a 720 MHz, β=0.2 slotted-iris that had been investigated at Karlsruhe in the mid-70s [4]; a 150 MHz, β=0.2 quarter-wave in use at the University of Washington [5]; and a 850 MHz, β=0.28 spoke cavity that was under development at ANL [2,6].

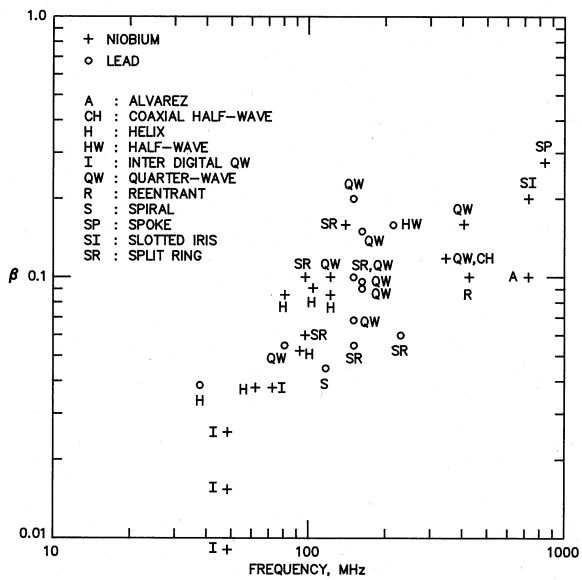

Figure 2: β<1 superconducting structures (circa 1989) [3].

Since then there has been considerable interest and activity in the area of medium-β superconducting cavities, most of it related to the development of spallation neutron sources [7-17]. Figure 3 is an update of Figure 2 that focuses on the region 0.1<β<1 and 100 MHz<f<1 GHz. In blue are the cavities that were already present in Figure 2 and in red are the ones that have been studied since then. As can clearly be seen the medium-β region has now received considerable interest.

* Supported by the U.S. DOE Contract No DE-AC05-84-ER40150
†delayen@jlab.org

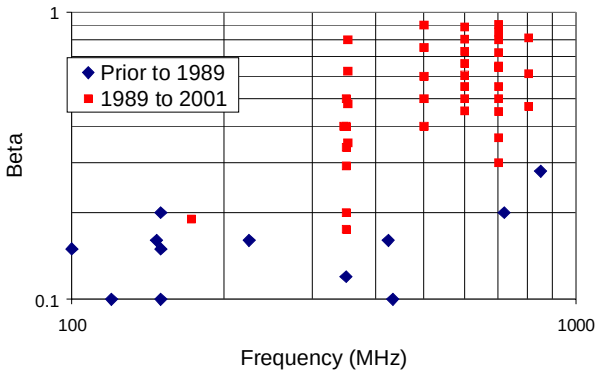

Figure 3: β<1 superconducting structures (circa 2001).

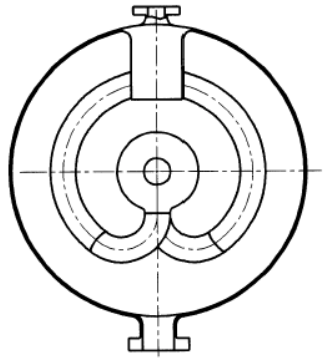

Figure 5: Concept of a 115 MHz, β=.13 for the RIA driver [22].

2 BASIC GEOMETRIES

The majority of the superconducting accelerating structures in use or under development, and applicable to the medium-β regime, fall under two broad categories: those based on a resonant transmission line mode (TEM-like) and those based on a Transverse Magnetic (TM) mode.

2.1 Resonant Transmission Line Modes

A large number of structures based on a TEM-like mode have been developed. They can be further separated into those using quarter-wavelength transmission lines and those using half-wavelength transmission lines.

The λ/4 structures can include a single loading element, as in the original quarter-wave [18], or several, as in the split-ring [19] or the twin quarter-wave [20] (improperly called a half-wave in the original paper).

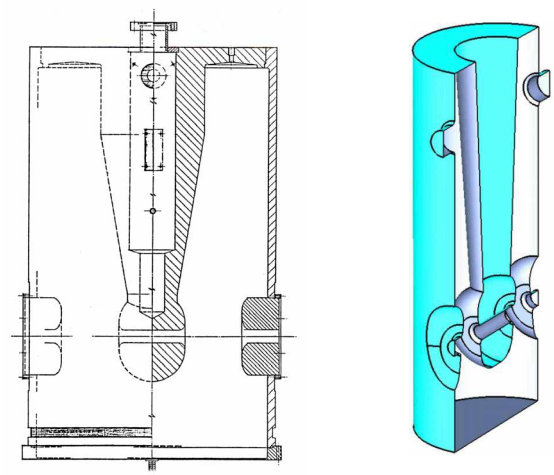

Figure 4: Quarter-wave resonators. Left: U. of Washington 150 MHz, β=0.2 [5]. Right: concept for a QW cavity for the RIA driver [21].

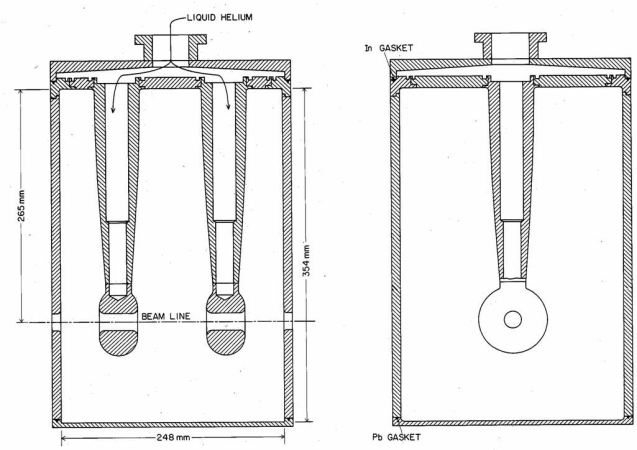

Figure 6: 225 MHz, β=0.16 twin quarter-wave resonator [20].

The λ/2 structures that have been developed and are under consideration for proposed applications are of two types: the coaxial half-wave [2, 23] and the spoke geometry [2, 6], the latter having the advantage of being able to be used as a building block for longer multi-gap structures [24, 25]. When the number of loading elements is large and they are rotated by 90° from one to the next, these cavities are sometime referred to as H-type cavities [28].

For the sake of completeness, other TEM-like superconducting structures that have been developed in the past, but do not seem to be attractive anymore, can be mentioned: the spiral (λ/4) and the helix (λ/2) resonators.

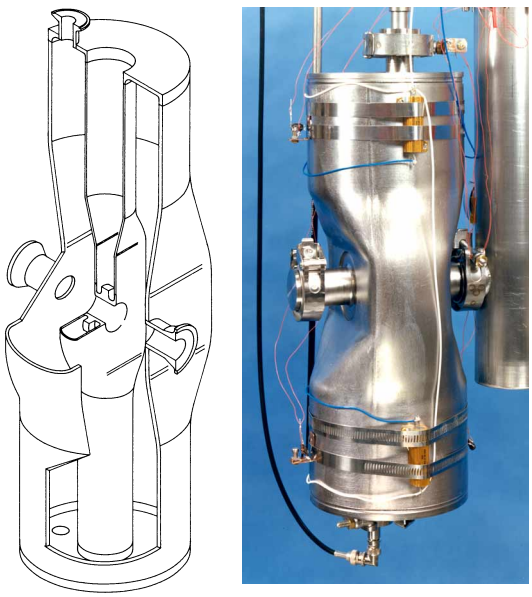

Figure 7: Concept and realization of a 350 MHz, β=0.12 coaxial half-wave resonator [2,23].

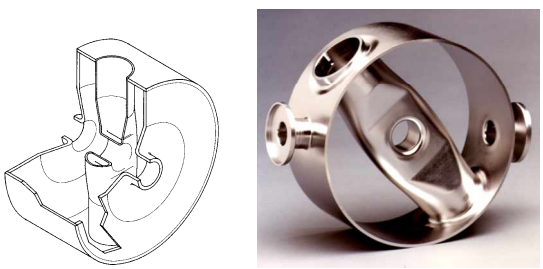

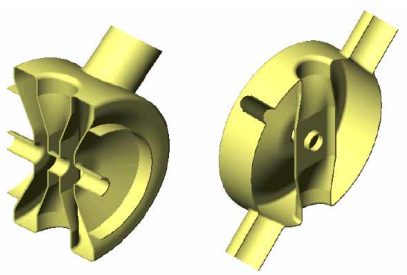

Figure 8: Single loading-element spoke cavities. Upper: 850 MHz, β=0.28 [2,6]. Middle: 350 MHz, β=0.4 [26]. Lower: 350 MHz, β=0.175 [27].

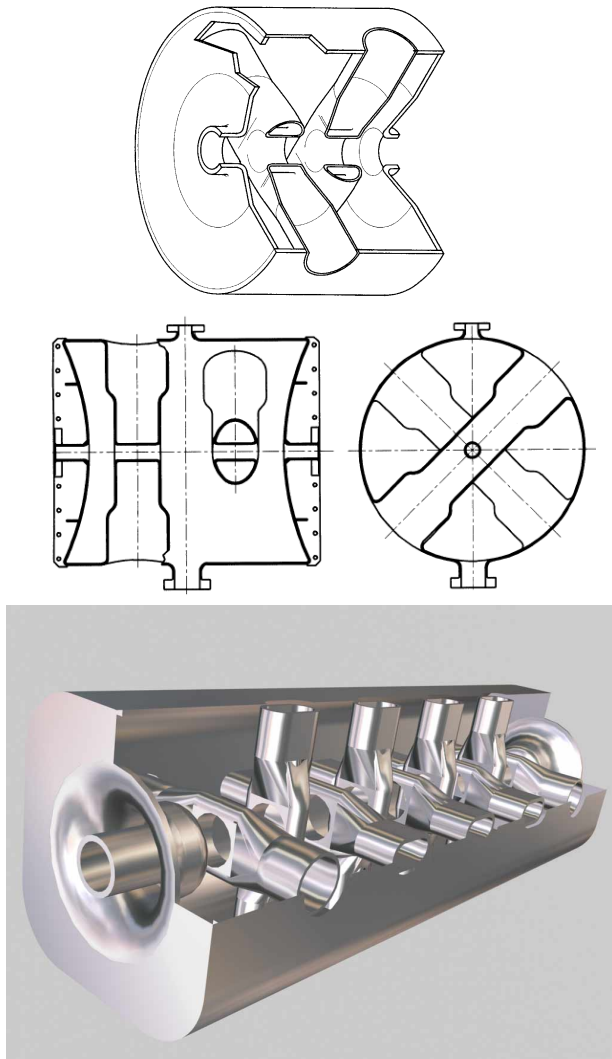

Figure 9: Concepts for multi-elements spoke cavities. Upper: 850 MHz, β=0.28 [24]. Middle: 345 MHz, β=0.4 [22]. Lower: 700 MHz, β=0.2 [28].

2.2 Transverse Magnetic Modes

All the superconducting cavities in operation today for velocity-of-light particles are of the same design with only subtle differences. They are of the so-called elliptical geometry, *i.e.* rounded pill-box cavities operating in the TM_{010} mode. This geometry can straightforwardly be extended to lower β by reducing the length of the cells while maintaining a constant frequency.

A number of TM mode cavities have been designed and tested for β's as low as 0.47. A few examples are shown below together with the reentrant cavity [29], which can be considered an extreme example of a TM cavity.

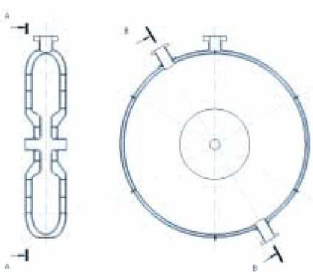

Figure 10: Examples of $\beta<1$ TM_{010} cavities. From top to bottom: 805 MHz, $\beta=0.82$ [30], 805 MHz, $\beta=0.62$ [30]; 700 MHz, $\beta=0.64$ [31]; 700 MHz, $\beta=0.47$ [32]; 352 MHz, $\beta>0.1$ [33].

3 BASIC PROPERTIES

The performance of superconducting cavities in, or their appropriateness to, various applications is captured by a few important properties or parameters. In this section we concentrate on these few properties for the cavity designs that are of interest for the medium-β region; in most cases these designs are of the $\lambda/2$ or the TM type and we will restrict ourselves to those two. The goal is not to present long lists of numbers for specific designs but to extract some general trends and dependencies for generic geometries. Whenever possible we will present simple β-dependencies or scaling laws.

Data have been gleaned from the literature and, although probably not complete, they are believed to be a fair representation of the properties of various structures.

Data for the TM cavities were obtained from [8, 25, 30-31, 34-39]. Data for the $\lambda/2$ cavities were obtained from [6, 22, 26, 27, 38, 40-42].

In many cases, for the TM geometry, families of cavities have been designed for various β and, in the graphs in the following sections, the data points belonging to a family will be joined by lines to indicate trends. As will be seen there are little differences between the various designs since the number of degrees of freedom in a TM geometry is quite limited.

In the case of $\lambda/2$ structures, however, no such families of similar designs of various β have been investigated and the data consist of isolated points, with a much larger scatter than in the case of TM structures due to the larger number of degrees of freedom in the design. For these structures a typical β-dependence of a particular parameter will be obtained from the formulae given in [43]. That paper refers to $\lambda/4$ structures, but the formulae can be easily adapted to $\lambda/2$ by assuming no loading capacitance and doubling the energy content and rf losses.

3.1 Peak Surface Electric Field

Until field emission has been fully eliminated, the ratio of peak surface electric field to accelerating field will remain one of the most important parameters characterizing superconducting structures.

For TM structures, the peak surface electric field occurs close to the iris. This ratio has a typical value of 2 for $\beta=1$, and increases slowly as the β is decreased to reach values of 3 to 4 for $\beta=0.5$.

For $\lambda/2$ structures, the peak surface electric field occurs at the center of the loading element and, by suitable sizing and shaping of its cross section to achieve a nearly constant surface field around the circumference, a typical ratio of 3.3 independent of β can be easily obtained. This is consistent with the experimental data, although higher values have been seen when the minimization of the surface electric field was not a driving consideration.

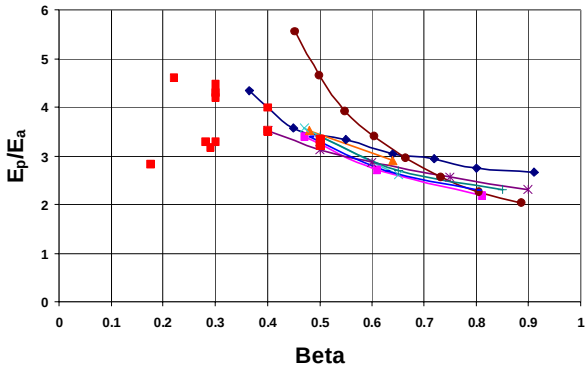

Figure 11: Ratio of peak surface to accelerating field. Data points joined by lines are for TM structures, isolated points (red squares) are for λ/2 structures.

3.2 Peak Surface Magnetic Field

The peak surface magnetic field is clearly another important parameter and will become increasingly so as the field emission limit is progressively raised. This parameter is often expressed as the ratio of peak surface magnetic field to accelerating field.

For TM structures the peak surface magnetic field occurs around the equator and, for β=1 structures, is typically 4 to 4.5 mT at 1 MV/m. This value increases slowly as β is lowered to reach 6 to 8 mT for β=0.5.

For λ/2 structures the maximum occurs where the loading element meets the outer enclosure and, again, is quite sensitive to the size and shape of the center conductor in that region. Nevertheless, typical values of 7 to 8 mT, independent of β, can be easily achieved. As in the case of the electric field, substantial deviations from that number can be obtained, depending on the particular design philosophy that was selected.

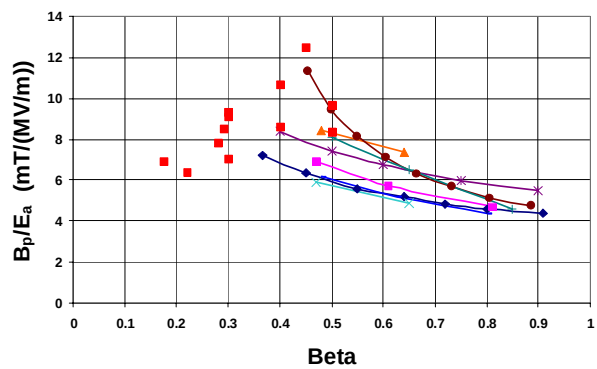

Figure 12: Ratio of peak surface magnetic to accelerating field. Data points joined by lines are for TM structures, isolated points (red squares) are for λ/2 structures.

3.3 Geometrical Factor (QR_s)

Another often-quoted parameter is the geometrical factor, or product of the quality factor and the surface resistance. This number (in Ω) is size and material independent and depends only on the shape of the structure.

The Q of a structure is proportional to the ratio of energy content to power dissipation. For TM structures, at constant frequency and electric field between the iris edges, the energy content should be roughly proportional to the volume (*i.e.* roughly proportional to β) while the power dissipation should be roughly proportional to the structure area, which, to first order, is independent of β. Thus, this simple argument indicates that, for TM structures, the geometrical factor should be nearly linear with β and, since it is typically of the order of 275Ω for β=1, a simple scaling law is $QR_s \approx 275\ \beta\ (\Omega)$. This scaling law is shown as a dashed blue line in the following figure and is consistent with the data. Note that the geometrical factor is independent of the number of cells.

For the λ/2 structures, a simple transmission line model similar to the one in [43] gives $QR_s \approx 270\ \beta\ (\Omega)$. This is shown as a dashed red line and is also consistent with the data. In this case, if we assume that most of the power dissipation takes place on the loading element, the geometrical factor is independent of the number of loading elements.

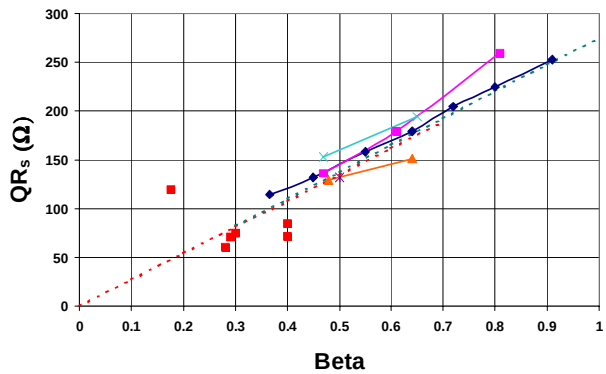

Figure 13: Geometrical Factor. Data points joined by lines are for TM structures, isolated points (red squares) are for λ/2 structures. Dashed blue and red lines are simple scaling laws (see text).

3.4 R_{sh}/Q

R_{sh}/Q, the ratio of the shunt impedance and the quality factor, is another parameter that depends only on shape and not on size or material. In this case however, for TM structures, this parameter is proportional to the number of cells and will be quoted per cell. As will be mentioned

later, in λ/2 structures unlike in TM structures, the cell-to-cell coupling is much stronger than the perturbation due to the beam port in the end cells, and the end cells are only half-cells (or half-gaps). This can be seen in figures 6 and 9. For this reason R_{sh}/Q is proportional not to the number of gaps but to the number of loading elements, and will be quoted per loading element.

Unfortunately this parameter is not quoted as often as the previous ones, especially for λ/2 structures. Additionally, there are several definitions for the shunt impedance, and the definition that is used is not always clearly defined in the publications; this reduces the amount of data that can be used.

The definition that will be adopted here for the shunt impedance is $R_{sh} = V^2/P$ where V is the energy gained by a particle of optimal velocity at crest of the rf phase and P is the power dissipation.

For TM structures one could use the same simple argument that was used for the geometrical factor and conclude that R_{sh}/Q per cell should be proportional to β. In this case the argument fails because the energy content and losses depend on the electric field at the iris diameter while the energy gain depend on the electric field on axis. As the β is reduced, the length of a cell becomes comparable to, or less than, the iris diameter. As a result, the on-axis field experienced by the particle is significantly reduced from the field between the cavity faces at the iris diameter that contributes to the losses; thus the structure becomes less efficient at transferring energy to the particle. For this reason, R_{sh}/Q decreases more rapidly than linearly and, from the published data, seems to decrease at least quadratically. A reasonable fit to the data seems to be $R_{sh}/Q \approx 120\ \beta^2\ (\Omega)$.

For λ/2 structures the same transmission line model mentioned before, applied to a "reasonable" geometry, gives $R_{sh}/Q \approx 205\ \Omega$ per loading element, independent of β. This is not inconsistent with the published data, although there is a large scatter in the data due to the many degrees of freedom in the structure design.

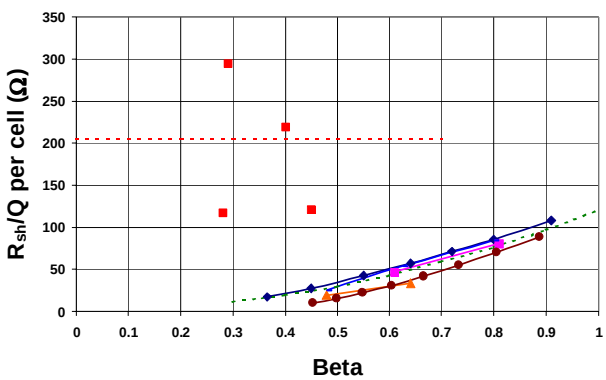

Figure 14: R_{sh}/Q per cell or loading element. Data points joined by lines are for TM structures, isolated points (red squares) are for λ/2 structures. Dashed blue and red lines are simple scaling laws (see text).

These simple models and the data indicate that, in the medium β region and possibly higher, the R_{sh}/Q of λ/2 structures is substantially higher than that of TM structures, typically a factor of 5 around β=0.5.

3.5 Shunt Impedance (R_{sh})

The shunt impedance, as defined above, is a direct measure of the power dissipation induced by the rf currents, and thus of the efficiency of a structure in accelerating particles. For superconducting structures it has a direct impact on the requirements for the cryogenic system. Since the shunt impedance is a material-dependent parameter, it can be made material-independent by presenting $R_{sh}R_s$, the product of the shunt impedance and the surface resistance of the cavity material. Alternatively, it is the product of R_{sh}/Q and QR_s, the two parameters defined above. $R_{sh}R_s$ (in Ω^2) depends only on the shape of the structure, not its size, and is proportional to either the number of cells or loading elements.

From the scaling laws found in 3.3 and 3.4 $R_{sh}R_s \approx 33000\ \beta^3\ (\Omega^2)$ for TM structures and $R_{sh}R_s \approx 55500\ \beta\ (\Omega^2)$ for λ/2 structures.

These scaling laws are consistent with the data, as shown in the following graph, although the published data gets scarce especially for the λ/2 structures. They indicate that the λ/2 structures require about 5 times less power dissipation than TM structures in the medium β region to produce a given energy gain (at a given frequency and length). This is a result of their smaller volume and concentration of high magnetic field in a smaller area.

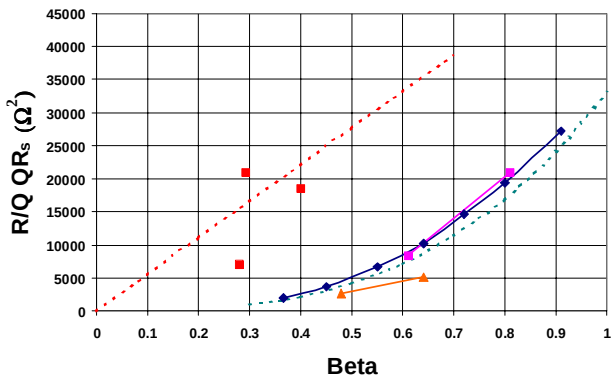

Figure 15: Product of shunt impedance and surface resistance (R_{sh} R_s) per cell or loading element. Data points joined by lines are for TM structures, isolated points (red squares) are for λ/2 structures. Dashed blue and red lines are simple scaling laws (see text).

3.6 Energy Content

The effect of the energy content is already included in the above parameters but is important in itself for the low current applications (such as RIA). When the beam loading is negligible, the amount of rf power involved in

phase stabilizing a structure at a given gradient with a given amount of detuning (microphonics) is given by the product of the energy content and the detuning. When stabilization is obtained by negative phase feedback the rf power that needs to be available from the rf source is $P = U \Delta\omega$ [44]. When stabilization is obtained *via* an externally controlled reactance the amount of reactive rf power that must be switched or controlled is given by $P = 4 U \Delta\omega$ [45].

Not only is the energy content proportional to the number of cells or loading elements but it also depends on the gradient and frequency as $U \propto E^2 \omega^{-3}$. The numbers quoted will be per cell or loading element, at 1 MV/m, and for a geometry scaled to 500 MHz.

The same simple argument that was used in 3.4 could be used to show that, for TM structures, the energy content should be linear with β, and it would be invalid for the same reason: as β is reduced, TM structures become less and less efficient at generating on-axis field from fields at the iris diameter. Data indicate that U at constant E_{acc} is roughly independent of β and may even increase as β decreases below 0.6-0.5. At typical number would be $U \approx 200$-250 (mJ).

For the $\lambda/2$ structures the same transmission line model predicts $U \approx 200\ \beta^2$ (mJ), which is consistent with the available data.

In this case one finds that the $\lambda/2$ structures have an energy content about 5 times lower than that of TM structures.

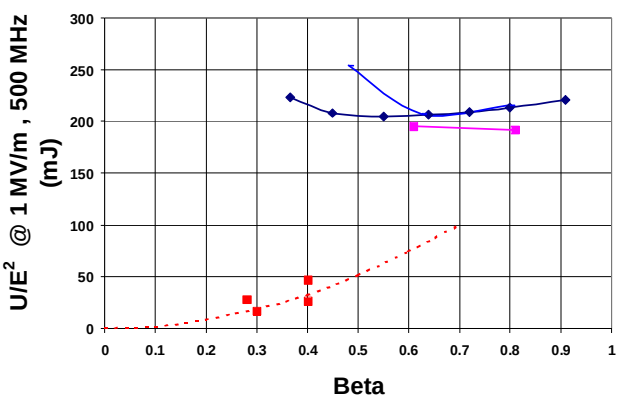

Figure 16: Energy content per cell or loading element at 1 MV/m for 500 MHz structures. Data points joined by lines are for TM structures, isolated points (red squares) are for $\lambda/2$ structures. The dashed red line is a simple scaling law (see text).

3.7 Size

One of the most striking differences between TM and $\lambda/2$ structures is in their transverse dimensions. Typically, TM cavities have an inside diameter between .88 and .92 λ. $\lambda/2$ structures, on the other hand have internal diameter between .46 and .51 λ, nearly a factor of 2 lower. This is shown in the following figure for 2 cavities of the same frequency and β. Thus a $\lambda/2$ cavity could be made much smaller (and lighter) at the same frequency, or (for roughly the same dimensions) at half the frequency, which means that for the same length it would have half the number of cells and thus a broader velocity acceptance and higher efficiency.

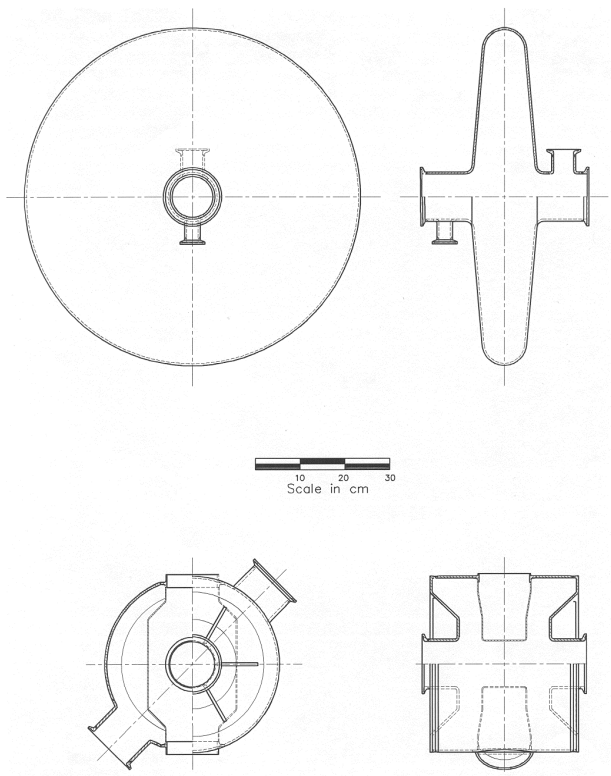

Figure 17: 350 MHz, β=0.45 structures. Upper: single-cell TM, lower: single-loading element $\lambda/2$ [7].

3.8 Cell-to-cell Coupling

In TM structures the cell-to-cell coupling typically takes place *via* the electric field through the irises. Increasing the iris diameter would increase the coupling but, at the same time, increase the peak surface electric field. For this reason the cell-to-cell coupling is usually of the order of 2 to 3 % or even less. The downside of a small cell-to-cell coupling is an increased sensitivity of the field flatness to mechanical deformation, which may be of particular concern for the medium β region. Since this coupling is small, it is of the order of the perturbation caused in the end-cells by the beam pipe. It is for this

reason that, in order to obtain a flat field profile in the π mode, the end-cells are nearly identical to center-cells instead of being half-cells.

For λ/2 structures the coupling does not rely on the beam holes but is done chiefly *via* the magnetic field that links all the cells through the openings. In this case the coupling is very strong (20 to 30%) which yields structures that are very robust with field profiles insensitive to mechanical tolerances. This strong coupling explains why the end-cells (end-gaps) are half-cells (half-gaps) in order to obtain a flat π mode.

3.9 Lorentz Detuning and Microphonics

It would be extremely difficult to present similar scaling laws for the Lorentz detuning coefficient (k_μ) and sensitivity to microphonics, as they are both intimately connected to the details of the mechanical design (material thickness, stiffening, *etc*,). However it is probably accurate to say, and it is borne out by experience, that λ/2 structures have lower k_μ and are less sensitive to microphonics than TM structures of similar frequency and β. For example, it has proven a challenge to design TM structures at 805 MHz and β's of .8 and .6 with $k_\mu < 4$ Hz/(MV/m)^2 [46]. A k_μ of 3.7 Hz/(MV/m)^2 was obtained on a single-element 350 MHz, β=0.4 spoke cavity [47]; and the 225 MHz, β=0.16 twin-quarter wave shown in figure 6 had a k_μ of 0.42 Hz/(MV/m)^2.

It is interesting to note that, for the TM cavities, the radiation pressure-induced deformation takes place in all the cells, and k_μ should be independent of the number of cells. For λ/2 structures, at least of the spoke type, most of the contribution comes from the deformation of the end plates, and thus k_μ should decrease as the number of loading elements is increased.

3.10 Multipacting

Multipacting has been an important limitation in the performance of superconducting cavities and, in the case of TM structures, has been virtually eliminated by the introduction of the "elliptical" geometry. Recently simulation tools have been developed that, for these structures that are fairly simple geometrically, allow the designer to predict and avoid the occurrence of multipacting [48].

The λ/2 structures, on the other hand, are fully 3-dimensional and we do not have, at present, reliable modeling tools for simulating and predicting multipacting. For this reason, among others, a prototyping step is recommended. Based on the large number of these types of structures that have been developed and tested so far, it can be said, with a reasonable degree of confidence, that multipacting will "always" occur but it will "never" be a showstopper. Sometimes it can take a few minutes to disappear, sometimes several hours, but, based on available information, no such structure has been permanently stopped by multipacting.

4 SUMMARY

Both the accelerating structures based on TM modes and on λ/2 resonant lines have positive and negative features. In this section we summarize the positive features for both of them:

4.1 TM Structures – Positive Features

- Geometrically simple
- Familiar
- Wide knowledge base, both in research institutions and in industry.
- Good design, modeling, and simulation tools
- Low surface fields at high β
- Small number of degrees of freedom in the design

4.2 λ/2 Structures – Positive Features

- Compact, small size
- High shunt impedance
- Robust, stable field profile (high cell-to-cell coupling)
- Mechanically stable (low Lorentz coefficient, microphonics)
- Small energy content
- Low surface fields at low β
- Large number of degrees freedom in the design.

5 ACKNOWLEDGEMENTS

Many thanks to all the colleagues who have provided information, data, or figures for this work; in particular G. Ciovati, K. W. Shepard, T. Tajima, and E. Zaplatin.

6 REFERENCES

[1] M. Kuntze, "Progress Report on Superconducting Proton Linacs," Proc. PAC'73, San Francisco, March 1973, p. 49.

[2] J. R. Delayen, "Superconducting Accelerating Structures for High-Current Ion Beams," Proc. LINAC'88, Newport News, October 1988, p. 199.
J. R. Delayen and C. L. Bohn, "Prototype Resonators for High-Current Ion Beams," Proc. 4th Workshop on RF Superconductivity, Tsukuba, August 1989, p. 427.

[3] J. R. Delayen, "Low-Velocity Superconducting Accelerating Structures," Proc. 4th Workshop on RF Superconductivity, Tsukuba, August 1989, p. 249.

[4] K. Mittag, "Superconducting Accelerating Structures for Medium Energy Protons," Proc. PAC'77, Chicago, March 1977, p. 1156.

[5] D. W. Storm, D. T. Corcoran, M. A. Howe, Q. –X. Lin, and D. P. Rosenzweig, " Status Report on the University of Washington Booster Accelerator Project," Proc. 3rd Workshop on RF Superconductivity, Argonne, September 1987, p. 367.

[6] J. R. Delayen, W. L. Kennedy, and C. T. Roche, "Design and Test of a Superconducting Structure for

High-Velocity Ions," Proc. LINAC'92, Ottawa, August 1992, p. 695.

[7] J. R. Delayen, C. L. Bohn, B. J. Micklich, C. T. Roche, and L. Sagalovsky, "Design Considerations for High-Current Superconducting Ion Linacs," Proc. PAC'93, Washington, May 1993, p. 1715.

[8] S. Aminov, A. Gamp, E. Haebel, H. Heinrichs, H. Piel, J. Pouryamout, Th. Schilcher, D. L. Schrage, G. Schulz, S. Simrock, C. H. Rode, and R. Roth, "Conceptual Design of the Superconducting High-Energy Linear H^- Accelerator for the Future European Spallation Source," **ESS-96-6--L**, December 1996.

[9] C. Pagani, G. Bellomo, P. Pierini, D. Barni, A. Bosotti, A. Martino, R. Parodi, S. Visona, "A 100-600 MeV High-Current SC Proton Linac for Waste Transmutation and Energy Amplification," Proc. 8th Workshop on RF Superconductivity, Abano Terme, October 1997, p. 36.

[10] B. Rusnak, K. C. Chan, B. Campbell, B. Gentzlinger, B. Haynes, F. Krawczyk, A. Shapiro, R. Bibeau, D. Montoya, B. Smith, R. Lujan, T. Hargenradter, D. Hammon, "High-Intensity Proton Linac Activities at Los Alamos," Proc. 8th Workshop on RF Superconductivity, Abano Terme, October 1997, p. 1.

[11] M. Mizumoto, J. Kusano, K. Hasegawa, N. Ouchi, H. Oguri, M. Kinsho, E. Chishiro, T. Tomisawa, Y. Touchi, M. Ikegami, Y. Honda, K. Mukugi, H. Ino, F. Noda, N. Akaoka, H. Kaneko, "A High Intensity Proton Linac Development for the JAERI Neutron Science Project," Proc. LINAC'98, Chicago, August 1998, p. 349.

[12] K. C. D. Chan, "Review of Superconducting RF Technology for High-Power Proton Linacs," Proc. 9th Workshop on RF Superconductivity, Santa Fe, November 1999, p. 465.

[13] H. Safa, "Superconducting Proton Linac for Waste Transmutation," Proc. 9th Workshop on RF Superconductivity, Santa Fe, November 1999, p. 357.

[14] K.W. Shepard, J. R. Delayen, C. M. Lyneis, J. Nolen, P. Ostroumov, J. W. Staples, J. Brawley, C. Hovater, M. Kedzie, M. P. Kelly, J. Mammosser, C. Piller, M. Portillo, "SC Driver for a rare Isotope Facility," Proc. 9th Workshop on RF Superconductivity, Santa Fe, November 1999, p. 345.

[15] S. Noguchi, "JAERI/KEK Joint Project," these proceedings.

[16] K. W. Shepard, "The U.S. RIA Project SRF Linacs," these proceedings.

[17] E. Chiaveri, "A High-Power Superconducting H^- Linac (SPL) at CERN," these proceedings.

[18] I. Ben-Zvi and J. M. Brennan, "The Quarter-Wave Resonator as a Superconducting Linac Element," **NIM 212** (1983) p. 73.

[19] K. W. Shepard, J. E. Mercereau and G. J. Dick, "A New Superconducting Heavy Ion Structure Using Chemically Polished Lead Surfaces," Proc. PAC'75.

[20] J. R. Delayen and J. E. Mercereau, "Cryogenic Test of a Superconducting Half-Wave Resonator for the Acceleration of Heavy-Ions," **NIM** A257 (1987) p. 71.

[21] K. W. Shepard, private communication.

[22] K. W. Shepard and T. E. Tretyakova, "Superconducting Accelerating Structures for a Multi-Beam Driver for RIA," Proc. LINAC'00, Monterey, August 2000, p. 920.

[23] J. R. Delayen, C. L. Bohn, and C. T. Roche, "Experimental Results in Superconducting Niobium Resonators for High-Brightness Ion Beam Acceleration," Proc. LINAC'90, Albuquerque, September 1990, p. 85.

[24] J. R. Delayen, C. L. Bohn, and C. T. Roche, "Application of RF Superconductivity to High-Brightness Ion Beam Acceleration," Proc. LINAC'90, Albuquerque, September 1990, p. 82.

[25] E. Zaplatin, "A Spoke Cavity Simulation with MAFIA," 9th Workshop on RF Superconductivity, Santa Fe, November 1999, p. 516.

[26] K. W. Shepard, M. Kedzie, J. R. Delayen, J. Mammosser, C. Piller, "Prototype 350 MHz, Niobium Spoke-Loaded Cavities," Proc. Proc. PAC'99 New York, March 1999, p. 955.

[27] F. L. Krawczyk, R. Garnett, R. P. LaFave, J. P. Kelley, D. L. Schrage, T. Tajima, " Design of a Low-β 2-Gap Resonator for the AAA Project," Proc. PAC'01, Chicago, June 2001.

[28] E. Zaplatin, "Electrodynamics and Mechanical Features of H-Type Superconducting Structures for Low Energy Part of ESS Linac," **ESS 116-01**-L, July 2001.

E. N. Zaplatin, "Low-β SC RF Cavity Investigations," these proceedings.

[29] P. H. Ceperley, I. Ben-Zvi, H. F. Glavish, and S. S. Hanna, "Superconducting reentrant Cavities for Heavy Ion Linacs," Proc. PAC'75.

[30] G. Ciovati P. Kneisel, J. Brawley, R. Bundy, I. Campisi, K. Davis, K. Macha, D. Machie, J. Mammosser, S. Morgan, R. Sundelin, L. Turlington, K. Wilson, M. Doleans, S. H. Kim, D. Mangra, D. Barni, C. Pagani, P. Pierini, K. Matsumoto, R. Mitchel, D. Schrage, R. Parodi, J. Sekutovicz, P. Ylae-Oijala, "Superconducting Prototype Cavities for the Spallation Neutron Source (SNS) Project," Proc. PAC'01, Chicago, June 2001.

[31] T. Tajima, K. C. Chan, R. C. Gentzlinger, W. B. Haynes, J. P. Kelley, F. L. Krawczyk, M. A. Madrid, D. I. Montoya, D. L. Schrage, A. H. Shapiro,, "Developments, of 700 MHz 5-Cell Superconducting Cavities for APT," Proc. PAC'01, Chicago, June 2001.

[32] C. Pagani, D. Barni, G. Bellomo, A. Bosotti, P. Michelato, R. Paulon, P. Pierini, D. Sertore, and G. Varisco, "Status of the High-Energy SC Linac for the TRASCO Program," Proc. PAC'01, Chicago, June 2001.

[33] A. Facco, V. Zviagintsev, and B. M. Pasini, "A Superconductive Low Beta Single Gap Cavity for a High Intensity Proton Linac," Proc. LINAC'00, Monterey, August 2001, p. 929.

[34] D. Barni, A. Bosotti, C. Pagani, P. Pierini, S. Visona, G. Gemme, R. Parodi, "SC Beta Graded Design for a

Proposed 350 MHz Linac for Waste Transmutation and Energy Production," Proc. EPAC'98, Stockholm, June 1998, p. 1870.

[35] C. Benvenutti, D. Boussard, S. Calatroni, E. Chiaveri, and J. Tuckmantel, "Production and Test of 352 MHz Niobium Sputtered Reduced Beta Cavities," Proc. 8th Workshop on RF Superconductivity, Abano Terme, October 1997, p. 1038.

[36] C. C. Compton, T. L. Grimm, W. Hartung, H. Podlech, R. C. York, G. Giovati, P. Kneisel, D. Barni, C. Pagani, and P. Pierini, "Niobium Cavity Development for the High-Energy Linac of the Rare Isotope Accelerator", Proc. PAC'01, Chicago, June 2001.

[37] N. Ouchi, J. Kusano, N. Akaoka, S. Takeuchi, B. Fechner, K. Hasegawa, M. Mizumoto, H. Inoue, E. Kako, S. Noguchi, M. Ono, K. Saito, K. Mukugi, and Y Honda, "Proton Linac Activities at JAERI," Proc. 8th Workshop on RF Superconductivity, Abano Terme, October 1997, p. 12.

[38] E. Zaplatin, W. Braeutigam, and S. Martin "Design Study for SC Proton Linac Accelerating Cavities," Proc. PAC'99, New York, March 1999, P. 959.

[39] J. L. Bariote, H. Safa, J. P. Charrier, S. Jaidane, H. Gassot, T. Junquera, J. Lesrel, G. Giovati, P. Pierini, D. Barni, and C. Pagani, "704 MHz, Superconducying Cavities for a High Intensity Proton Accelerator," Proc. 9th Workshop on RF Superconductivity, Santa Fe, November 1999, p. 384.

[40] K. W. Shepard, M. Kedzie, M. P. Kelly, and T. Schultheiss, "Superconducting Intermediate-Velocity Drift-Tube Cavities for the RIA Driver Linac," Proc. PAC'01, Chicago, June 2001.

[41] T. Tajima, K. C. D. Chan, R. C. Gentzlinger, W. B. Haynes, J. P. Kelley, F. L. Krawczyk, R. P. LaFave, M. A. Madrid, D. I. Montoya, D. L. Schrage, A. H. Shapiro, and K. W. Shepard, "Evaluation and Testing of a Low-β Spoke Resonator", Proc. PAC'01, Chicago, June 2001.

[42] E. Zaplatin, "Design of Superconducting RF Accelerating Structures for High Power Proton Linac," ESS 104-00-A, July 2000.

[43] J. R. Delayen, "Design of Low Velocity Superconducting Accelerating Structures Using Quarter-Wavelength Resonant Lines," **NIM** A259, (1987), 341-357.

[44] J. R. Delayen, G. J. Dick, and J. E. Mercereau, "A Microprocessor-Based Feedback System for Phase and Amplitude Stabilization of Superconducting Resonators", Proc. PAC'77, Chicago, March 1977 p. 1759.

[45] J. M. Bogaty, B. E. Clifft, K. W. Shepard, and G. P. Zinkann, "An Improved Phase-Control System for Superconducting Low-Velocity Accelerating Structures," Proc. PAC'89, Chicago, March 1989, p. 1978.

[46] G. Ciovati, P. Kneisel, J. Brawley, R. Bundy, I. Campisi, K. Davis, K. Macha, D. Machie, J. Mammosser, S. Morgan, R. Sundelin, L. Turlington, H. Wang, K. Wilson, M. Doleans, S. H. Kim, D. Mangra, D. Barni, C. Pagani, P. Pierini, K. Matsumoto, R. Mitchel, D. Schrage, R. Parodi, J. Sekutovicz, P. Ylae-Oijala, "Superconducting Prototype Cavities for the Spallation Neutron Source (SNS) Project," these proceedings.

[47] K.W. Shepard, private communication.

[48] W. Hartung, F. Krawczyk, H. Padamsee, "Studies of Multipacting in Axisymmetric Cavities for Medium-Velocity Beams," these proceedings.